

CONF-9510106--1

UCRL-JC-121678
PREPRINT

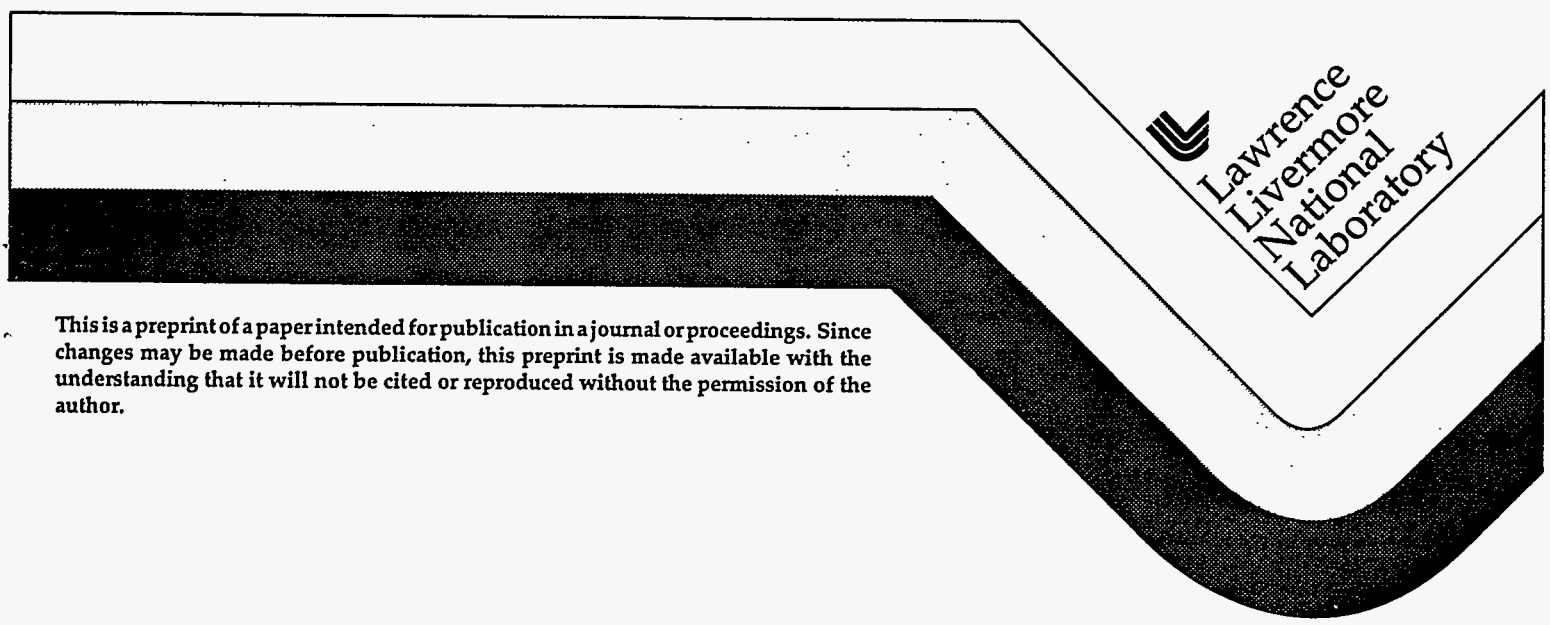
Optical Tuning a Dichroic Multilayer for a High Fluence Laser Application

RECEIVED
JAN 16 1995
OSTI

R. Chow
G. E. Loomis
C. Bibeau
N. E. Molau
V. K. Kanz
R. J. Beach

This paper was prepared for submittal to the
Annual Symposium on Optical Materials for High Power Lasers
Boulder, CO
October 30-November 1, 1995

October 11, 1995



This is a preprint of a paper intended for publication in a journal or proceedings. Since changes may be made before publication, this preprint is made available with the understanding that it will not be cited or reproduced without the permission of the author.

DISTRIBUTION OF THIS DOCUMENT IS UNLIMITED *OK*

MASTER

DISCLAIMER

This document was prepared as an account of work sponsored by an agency of the United States Government. Neither the United States Government nor the University of California nor any of their employees, makes any warranty, express or implied, or assumes any legal liability or responsibility for the accuracy, completeness, or usefulness of any information, apparatus, product, or process disclosed, or represents that its use would not infringe privately owned rights. Reference herein to any specific commercial product, process, or service by trade name, trademark, manufacturer, or otherwise, does not necessarily constitute or imply its endorsement, recommendation, or favoring by the United States Government or the University of California. The views and opinions of authors expressed herein do not necessarily state or reflect those of the United States Government or the University of California, and shall not be used for advertising or product endorsement purposes.

Optical tuning a dichroic multilayer for a high fluence laser application*

Robert Chow, Gary E. Loomis, Camille Bibeau, Nicole E. Molau, Vernon K. Kanz, and Raymond J. Beach

Lawrence Livermore National Laboratory
P. O. Box 808, Livermore, California 94551

ABSTRACT

We report on the design and successful fabrication of a dichroic multilayer stack using a procedure that allowed shifting from high reflectance to high transmittance within 89 nm and surviving high laser fluences. A design approach based on quarter-wave thick layers allowed the multilayer stack to be optically tuned in the last layers of the stack. In our case, this necessitated removing the samples from the coating chamber for a transmittance scan prior to depositing the last layers. This procedure is not commonly practiced due to thermal stress-induced failures in an oxide multilayer. However, D. J. Smith and co-workers reported that reactive e-beam evaporated hafnia from a Hf source produced laser-resistant coatings that had less coating stress compared to coatings evaporated from a HfO₂ source. Tuned dichroic coatings were made that had high transmittance at 941 nm and high reflectance at 1030 nm. The coating was exposed for 5 minutes to a 100 kW/cm² 1064 nm (180-ns pulsewidth, 10.7 kHz) laser beam and survived without microscopic damage. The same coating survived a 140 kW/cm² of laser intensity without catastrophic damage before optical tuning was performed.

Keywords: dichroic, e-beam evaporation, hafnium dioxide, laser damage, optical design

1. INTRODUCTION

Laser diode arrays can extend the operating life cycle of solid state lasers as flashlamp substitutes. High average power diode pumped solid state lasers (DPSSLs) have uses in electronic and materials processing, atmospheric and space-based LIDAR systems, underwater illumination and sensing, wind shear sensing, remote sensing of chemical species, lithographic processing, and medical tools. Diode pumped solid state lasers can also be easily coupled to fiber optic systems. Fabrication and packaging issues of high power DPSSLs have been addressed at Lawrence Livermore National Laboratory (LLNL). A simple end-pumping architecture has successfully delivered pump powers as high as 35 kW/cm² (2.5 kW on a 3 mm diameter rod). The architecture can be scaled in absolute power to intensities approaching 100 kW/cm².¹

A critical component of high-powered DPSSL systems are the dichroic coatings required on ends of the laser rod. One optical coating specification for a DPSSL with a Yb-doped Y₃Al₅O₁₂ (Yb:YAG) rod is a 941 nm high transmittance (HT) and a 1030 nm high reflector (HR) on the pump end, and the conjugate coating on the opposite, output end. Based on the emission and pump cross-sections of Yb, the average circulated intracavity intensity was calculated to be 56 kW/cm² with a 180-ns pulsewidth.

Fabricating high laser damage coatings for these applications bring about two issues of concern. First, multilayers made from a reactive Hf process have low damage thresholds in a 355 nm high peak power laser system. We believe that the HfO₂ absorption increases from the use of a metallic Hf source and becomes apparent at wavelengths shorter than 1064 nm. Although the design wavelength for our dichroic is near 1064 nm, optical multilayers made with the Hf process have yet to be tested in high average power applications. The damage mechanisms of high average power lasers is not clear, but may include absorption mechanisms. Second, the dichroic specifications require the multilayer to switch its function as a HR to a HT within 90 nm. Humidity- and temperature-induced shifts in the multilayer performance must be accounted for. A design approach based on quarter-wave thick layers allowed the multilayer stack to be optically tuned in the last layers of the stack. In our case, the samples were removed from the coating chamber, the transmittance measured, and returned to the chamber for deposition of the last layers. This procedure is not commonly practiced due to thermal stress-induced failures in a thick oxide multilayer. However, D. J. Smith and co-workers² reported that reactive e-beam evaporated HfO₂ from a metallic Hf source produced laser-resistant coatings that had less coating stresses than that from a HfO₂ source. The pump-end coatings have been made with this process and damage tested.

* This work was performed under the auspices of the U. S. Department of Energy by Lawrence Livermore National Laboratory under contract No. W-7405-Eng-48.

2. DICHOIC COATING PROCEDURE

2.1 Sample preparation

Undoped YAG rod (1 cm in diameter x 10 cm long) were purchased commercially.³ From this rod, substrate coupons were cut, polished, and finished at LLNL to 2 mm thicknesses. The surface finish was specified scratch/dig of 10/5, parallelism between the faces were < 10 seconds of an arc, sides were finished with < 30 μm grit, and the edges chamfered.

The two options for generating an optical design were to use either a computer-optimized or a basic quarter-wave design. The computer-optimized designs easily met the required optical specifications. However, these designs seldom had layer thicknesses based on one reference wavelength and required precise thickness control to meet the specifications. These designs would have been more difficult to make using a reactive e-beam deposition process as compared to making a basic quarter-wave design.

Therefore, we selected the quarter-wave design strategy, which had the advantage of allowing for optical tuning and thus an added assurance of meeting the design specifications. The quarter-wave design was $\text{YAG}/(\text{HL})^{12} \text{H} 0.5 \text{L}/\text{Air}$, where H is a quarter-wave optically thick HfO_2 layer, L is a quarter-wave optically thick SiO_2 layer, and the reference wavelength is 1110 nm. The layer sequence for tuning was (0.5L H 0.5L). Dichroic coatings, HT at 941 nm and HR at 1030 nm, were made on two samples. Sample 1 will be labeled 1a and 1b to designate the untuned and tuned stack, respectively. Sample 2 did not undergo the tuning procedure.

A reactive e-beam process was used to evaporate Hf (nominally 99.9% purity) to deposit HfO_2 layers and SiO_2 chips to deposit SiO_2 layers. Thicknesses were monitored optically as well as physically. The deposition rate for HfO_2 was 2 $\text{\AA}/\text{s}$ and for SiO_2 it was 5 $\text{\AA}/\text{s}$. The substrates were heated to and kept at $\approx 200^\circ\text{C}$ during the deposition process. A single layer SiO_2 anti-reflective coating (1030 nm) was deposited on the second surface of the substrate. The coating chamber was cyro-pumped and obtained base pressures of 2×10^{-7} Torr. The reactive O_2 pressure was 1.5×10^{-4} Torr and 5×10^{-5} Torr during Hf and SiO_2 evaporation, respectively.

2.2 Optical designs for tuning

As examples of optical tuning, computer simulated long- and short-wavelength pass optical designs were generated (Figs. 1 and 2, respectively). Both designs are based on a quarter-wave thicknesses of a single wavelength. In the long-pass case, the HT valley was centered at 1030 nm for a $(\text{HL})^9 \text{H}$ stack and HR peak that included 941 nm, where the reference wavelength was 892 nm. The HT valley was tuned to a longer wavelength (1040 nm) by adding a low index layer. To obtain a shift to a shorter wavelength (1023 nm), a low/high layer-pair was needed. For the curves shown in Fig. 1, the wavelength of the optical monitoring filter was not changed. The reference filter for optical monitoring could have been changed if finer tuning was needed. Therefore, in a long-pass design, the coater initially deposits for the targeted transmittance and then tunes the stack to shorter or longer wavelengths as required.

In the short-pass case (Fig. 2), the basic design was $(\text{HL})^9 \text{H} 0.5\text{L}$, where the reference wavelength was 1059 nm. The addition of a (0.5L H 0.5L) layer sequence shifted the HT valley from 930 nm to 937 nm and a second sequence shifted the stack to the targeted value of 941 nm. The design did allow tuning to shorter wavelengths by depositing a 0.5L over-layer but the sideband ripples become sharper. The coater would probably deposit slightly thinner layers and then adjusts to the longer (targeted) wavelength at the end of the stack.

In this work, we focused on the short-pass case for a high average power application. The coating process was interrupted in the 26th layer, the sample cooled down, removed from the coating chamber for a transmittance scan (Fig. 3, solid trace), and returned to the coating chamber for an additional (0.5L H 0.5L) deposition at 200°C . The coating was $\approx 4.4 \mu\text{m}$ thick when it was exposed to the deposition temperature cycle. There were no special temperature ramps applied during this procedure. The addition of a layer pair shifted the HT peak to the specified 941 nm wavelength (Fig. 3, dotted trace).

3. LASER DAMAGE

3.1 Test facility

In Fig. 4, we show a diagram of the experimental set-up used for laser damage testing of the multilayered stacks. A high power Q-switched Nd:YAG operating at a 10.7 kHz repetition rate with a pulsewidth of 180 ns was used to generate 128 W of 1064 nm laser light. The output beam emerging from the Nd:YAG system was elliptical with $1/e^2$ beam diameters of 3.9

mm and 2.6 mm or an average diameter of 3.3 mm. For simplicity, all average $1/e^2$ diameters will be used. A 5 cm positive lens was used to focus the beam to a 311 μm diameter spot size. The energy was measured with a Lab Master 2000 meter (5% accuracy). The incident energy, through the uncoated lens, was 107 W and the average power leakage through the samples were between 0.4 W and 0.7 W at 1064 nm. The samples were placed very close to the lens and then gradually moved towards the beam focus in order to increase the intensity up to 140 kW/cm².

3.2 Results and discussion

Sample 1a did not damage catastrophically at best focus. We also tested Sample 1a for damage in several different locations at best focus. In two of these locations, Sample 1a was irradiated for 5 minutes at 140 kW/cm². Sample 2 did not damage at an average intensity 32 kW/cm². The average beam diameter was 653 μm at this intensity. However, between 32 and 140 kW/cm², Sample 2 fractured. We have future plans to damage test additional samples to identify possible mechanisms. Based on the positive, preliminary laser damage test results on Sample 1a, we returned the sample to the coating chamber for the final optical tuning steps. Micrographs of Sample 1b were taken at 100x magnification before and after laser irradiation at 100 kW/cm² (5 minute exposure time) showed no microscopic damage from the laser test. Unfortunately, we were not able to test Sample 1b at higher intensities due to the unavailability of the test facility.

Although we are uncertain to the cause of damage in Sample 2, we are aware that laser-induced damage in dielectric multilayers typically occurs at coating defects. Of the two most common oxides used in high laser damage threshold optical multilayers, HfO₂ and SiO₂, it is the HfO₂ layers that limit the damage thresholds. This is because the major source of coating defects are generated during the reactive e-beam deposition process of HfO₂ layers.

It has been reported that there is a defect generation mechanism based on the volume change accompanying the HfO₂ solid-state phase transition at 1700°C.⁴ Evaporation of HfO₂ consists of sweeping a focused electron beam (e-beam) into a hearth of HfO₂ pellets. Impingement of the e-beam onto the top-most, exposed HfO₂ pellets heats them up to $\approx 2700^\circ\text{C}$, the melting temperature. There is a 1700°C temperature isotherm within the temperature profile of the HfO₂ source (from the top of the HfO₂ source at 2700°C down to the water-cooled hearth at 100°C). The fact that the e-beam continuously sweeps across the top of the HfO₂ source during the evaporation also means that the 1700°C isotherm is moving within the HfO₂ source. As a brittle oxide, the HfO₂ accommodates the volume changes by fracturing. So during HfO₂ evaporation, the source is continuously cracking and ejecting HfO₂ particulates. These particulates have been proven to seed the growth of the defects in coatings.⁵

A method to reduce the defect density in HfO₂ layers was to evaporate from metallic Hf instead of the oxide. The metal does not have a solid state phase transition nor the entrapped gasses of a HfO₂ source (which may also be another contributing source of defect seeds). Recent HRs made at LLNL and polarizers made by the University of Rochester showed that the defect density was reduced and the 1064 nm (high peak power, 3-ns pulse widths) damage thresholds significantly increased by switching from the conventional HfO₂ process to the metallic Hf process.⁶ We have demonstrated that this process also produces high damage threshold coatings for 1064 nm laser light with 180-ns pulsewidths (10.7 kHz).

In order to understand another reason why Sample 1 may have survived the high laser damage thresholds, we looked at the effect on E-fields from light incident on a nodular defect. The earlier E-field modeling in hafnia-seeded nodular defects were performed as light enters through the air/cone interface first.⁷ In this case, light enters from the air/YAG interface (1 GW/cm²), through the substrate, and then into the seed end of a nodular defect. The defect geometry chosen was a seed with a 0.73 μm diameter, buried 1.972 μm deep from the air/stack interface (total HR stack thickness was 3.90 μm), and was composed of HfO₂. Given this geometry and assuming omni-directional deposition, the cone diameter at the top of the stack was 1.7 μm . Two standing wave electric fields are shown in Fig. 5, one for an ideal stack (top trace) and another along the center axis of the nodular defect (bottom trace). The local E-field maxima decreased as 1064 nm light progresses into the stack (dashed and solid lines, respectively). In the ideal stack, the local E-field maxima decayed to some nominal value as light progresses through the entire stack. In the defect case, the E-fields were enhanced when light encountered the seed. However, the fields had sufficiently decayed to the point that the defect-induced field enhancement was less than the E-field maxima in the first HfO₂ layer exposed to the light. The local E-field maxima continued to decay as light passed through the seed and stack. Further modeling is required for seeds near the stack/substrate interface since this appeared to be the worst case scenario for our application.

In contrast, Ref.7 calculated a factor of 2.2 field enhancement for the defect geometry given above. For a seed range from 0.25 to 0.73 μm and a seed depth range from 1.33 to 2.61 μm , there was always an E-field enhancement as light initially

impinges on the cone part of the defect. When light enters from the seed end first, the defects appear less susceptible to laser damage given that the seeds were located in the stack-half nearest the air/stack interface, because there was no E-field enhancement.

4. CONCLUSIONS

We have designed and made a laser-resistant dichroic coating for a diode-pumped Yb:YAG based laser system. The dichroic shifted from high transmittance at 941 nm to high reflectance at 1030 nm. One coated sample survived laser intensity of 140 kW/cm² (180-ns pulsewidth) for 5 minutes. The sample was then tuned optically and survived intensities up to 100 kW/cm². Future work includes lifetime tests on coated Yb:YAG rods. Establishing such a high average power laser damage threshold opens up other avenues for high intensity DPSSLs. For instance, DPSSLs using Yb:S-FAP laser rods can be considered.

Fabrication of laser-resistant coatings based on quarter-wave designs have the advantage of optical tuning. Another development avenue is to determine whether oxide deposition from other e-beam evaporated metallic sources would provide lower stressed coatings.

5. ACKNOWLEDGEMENTS

We appreciate W. Kruepe and W. Ruvalcaba for their encouragement and support, J. Conrad for editing the manuscript, W. Eickelberg for use of the metrology lab, P. Thelin for fabricating the substrates, and G. Wilke for helping in the damage testing.

6. REFERENCES

1. R. J. Beach, M. A. Emanuel, W. J. Bennett, B. J. Freitas, D. Ciarlo, N. S. Carlson, S. B. Sutton, J. A. Skidmore, R. W. Solarz, Applications of Microlens-conditioned Laser Diode Arrays, SPIE 2383 (1995) 283-297.
2. D. J. Smith, J. F. Anzellotti, A.W. Schmid, S. Papernov, Z. R. Chrzan, and S. J. Vam Kerkhove, "Damage Fluence at 1054 nm and 351 nm of coatings made with hafnium dioxide evaporated from metallic Hf," Laser-induced damage in optical materials: 1994, SPIE v2428, 319.
3. Scientific Materials Corp., Bozeman, Montana.
4. R. Chow et al., Reactive evaporation of low-defect density hafnia, Applied Optics, 32 (1993) 5567-5574.
5. R. J. Tench, R. Chow, M. R. Kozlowski, "Characterization of defect geometries in multilayer optical coatings," J. Vac. Sci. Technol., A12 (Sep. 1994) 2808-2813.
6. F. Rainer, private communications.
7. J. F. DeFord and M. R. Kozlowski, Modeling of Electric Field Enhancement at Nodular Defects in Dielectric Mirror Coatings, Laser-induced Damage in Optical Materials: 1992, SPIE vol. 1848, pp. 455-473.

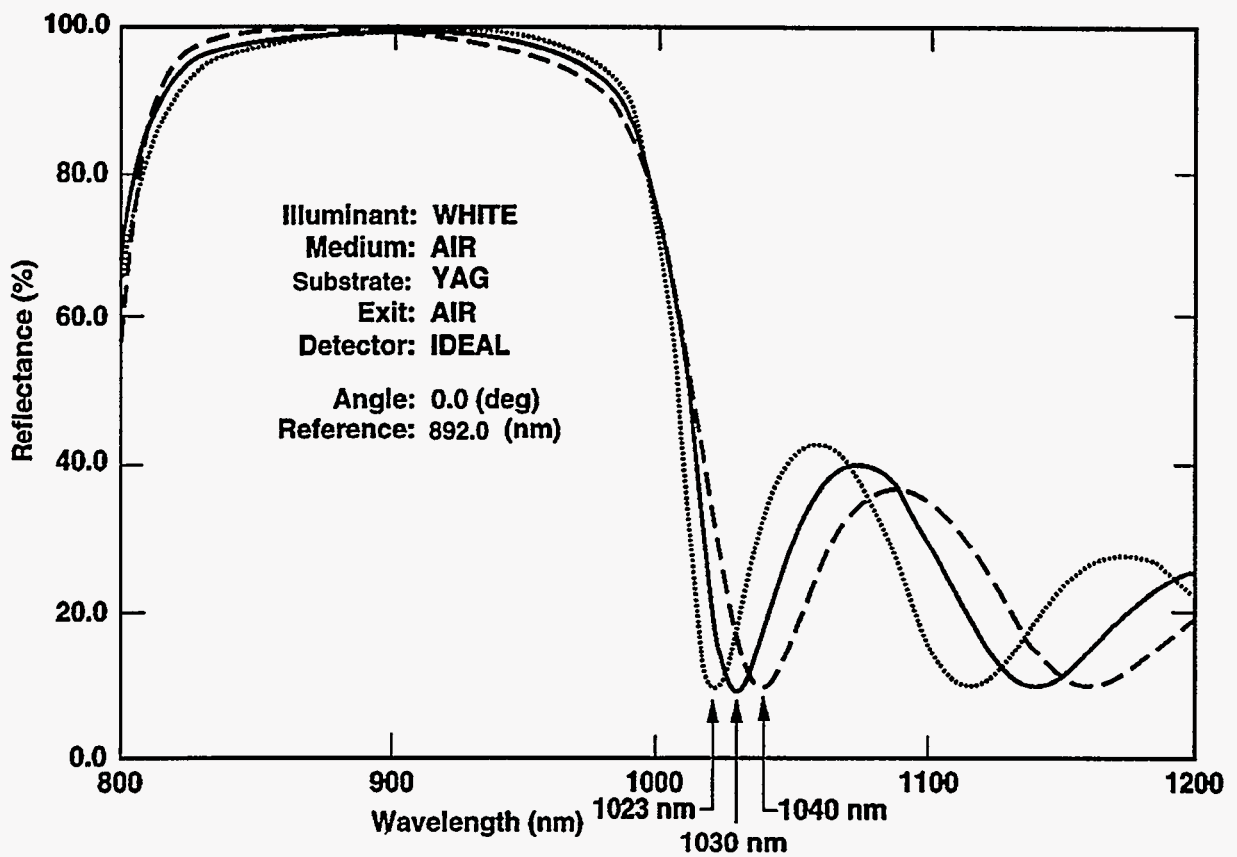


Figure1: Computer-generated optical tuning for a long-wave pass stack. The initial design is (HL)⁹ H and the high transmittance peak is located at 1030 nm (bold line). Subsequent addition of a L layer tuned the transmittance peak to a longer wavelength, 1040 nm. An addition of a (HL) layer-pair on top of the initial design tuned the transmittance peak to a shorter wavelength, 1023 nm.

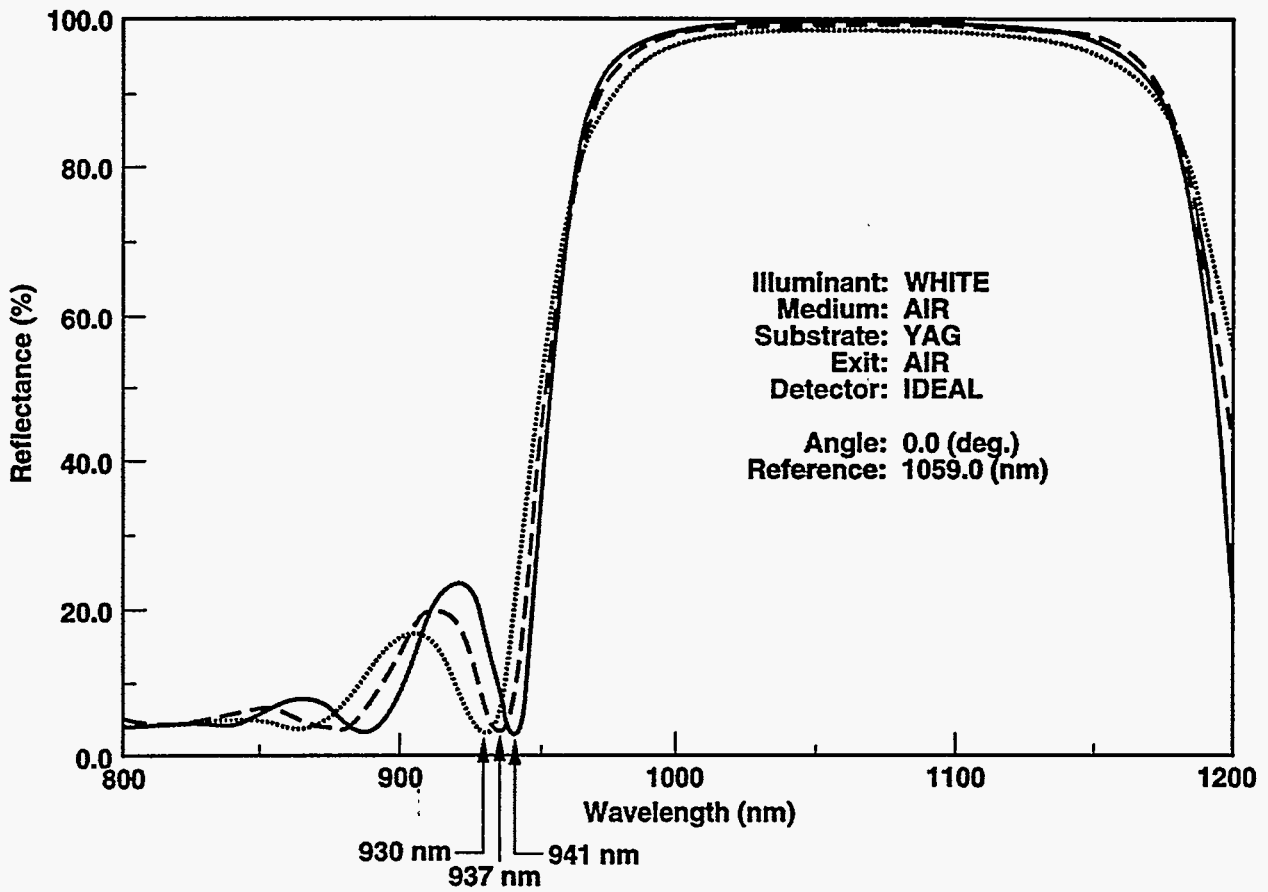


Figure 2: Computer-generated optical tuning for a short-wave pass stack. The initial design is $(HL)^9 H 0.5L$ and the high transmittance peak is located at 930 nm. Two subsequent additions of $(0.5L H 0.5 L)$ layers tuned the transmittance peak to 937 nm and finally to 941 nm (bold line).

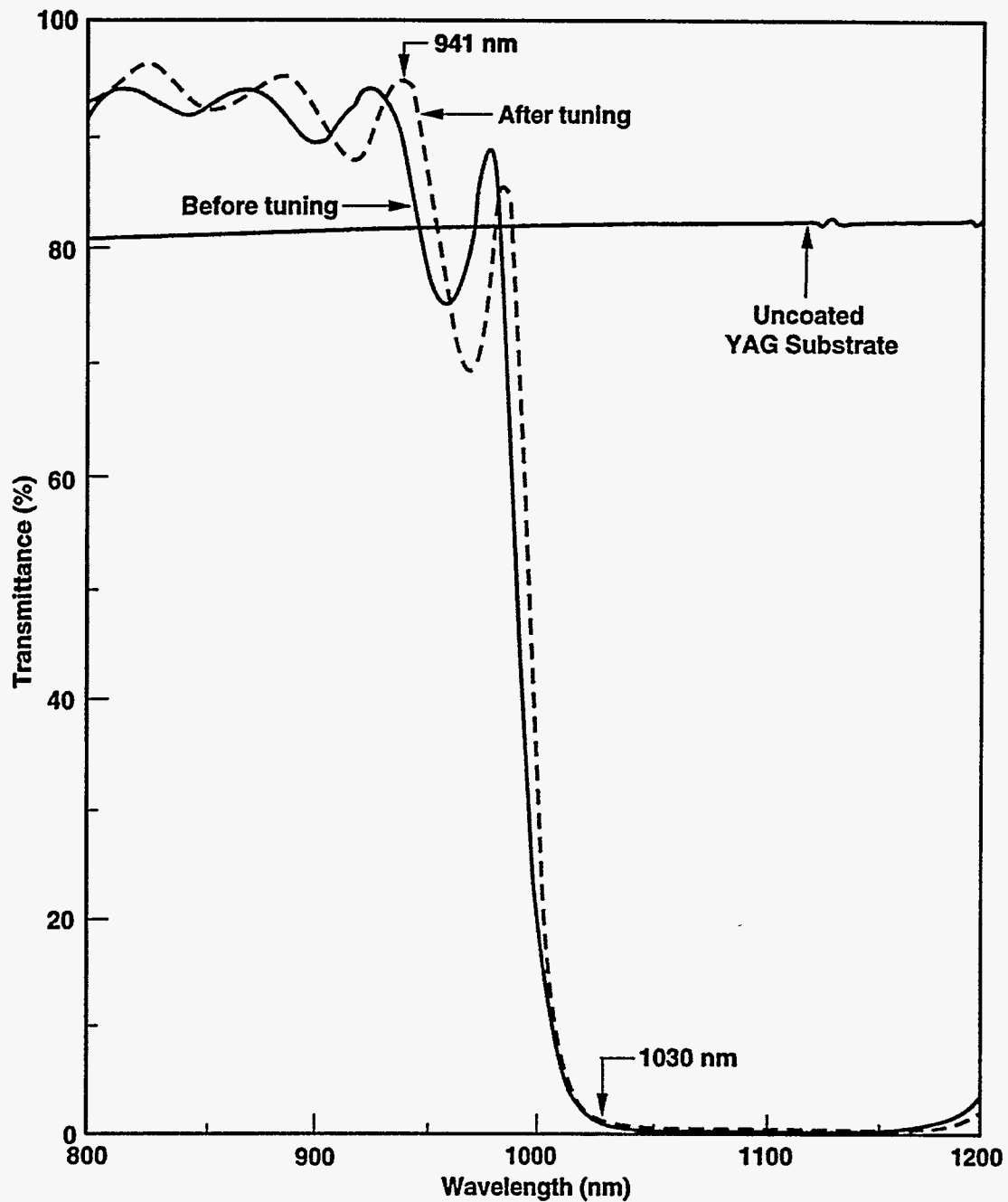


Figure 3: Transmittance scans during tuning of an optical stack. The solid trace was Sample 1a with the stack design $(HL)^{12} H 0.5L$. The dotted trace was Sample 1b, Sample 1a with an additional $(0.5L H 0.5L)$ layer sequence. The additional layer sequence increases the slope, thus bringing up the HT peak to 941 nm. The transmittance through an uncoated YAG substrate is shown for reference.

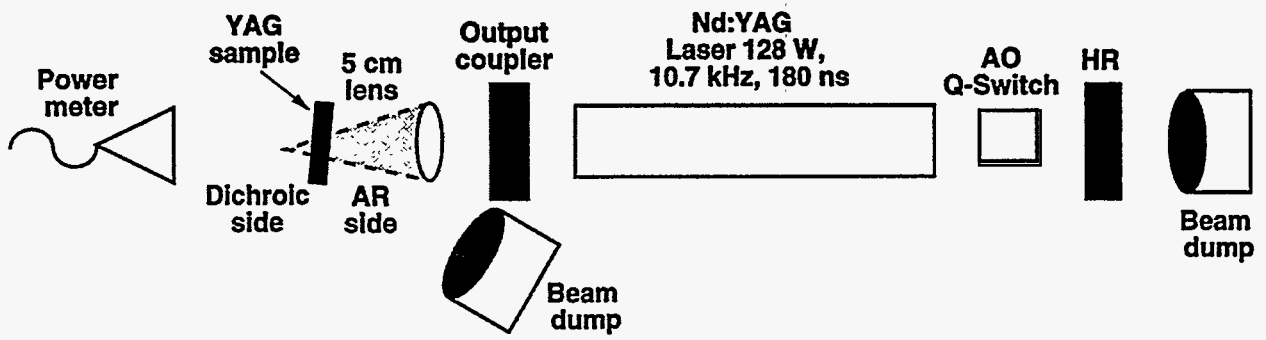


Figure 4: Experimental set-up for the laser damage testing at 1064 nm, 180 ns pulsewidth, 10.7 kHz. Laser light enters on the anti-reflective side of the sample to test the dichroic coating.

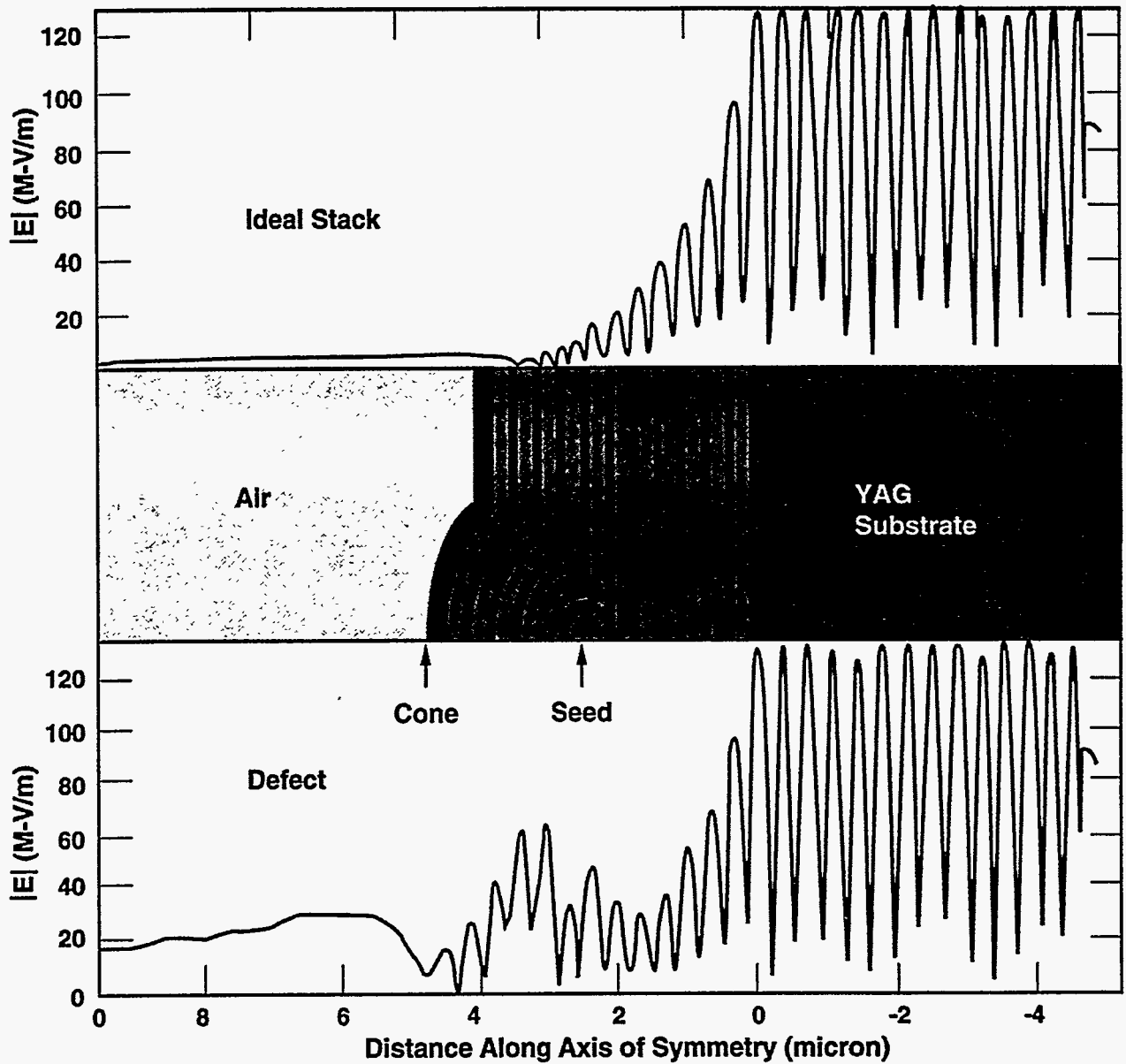
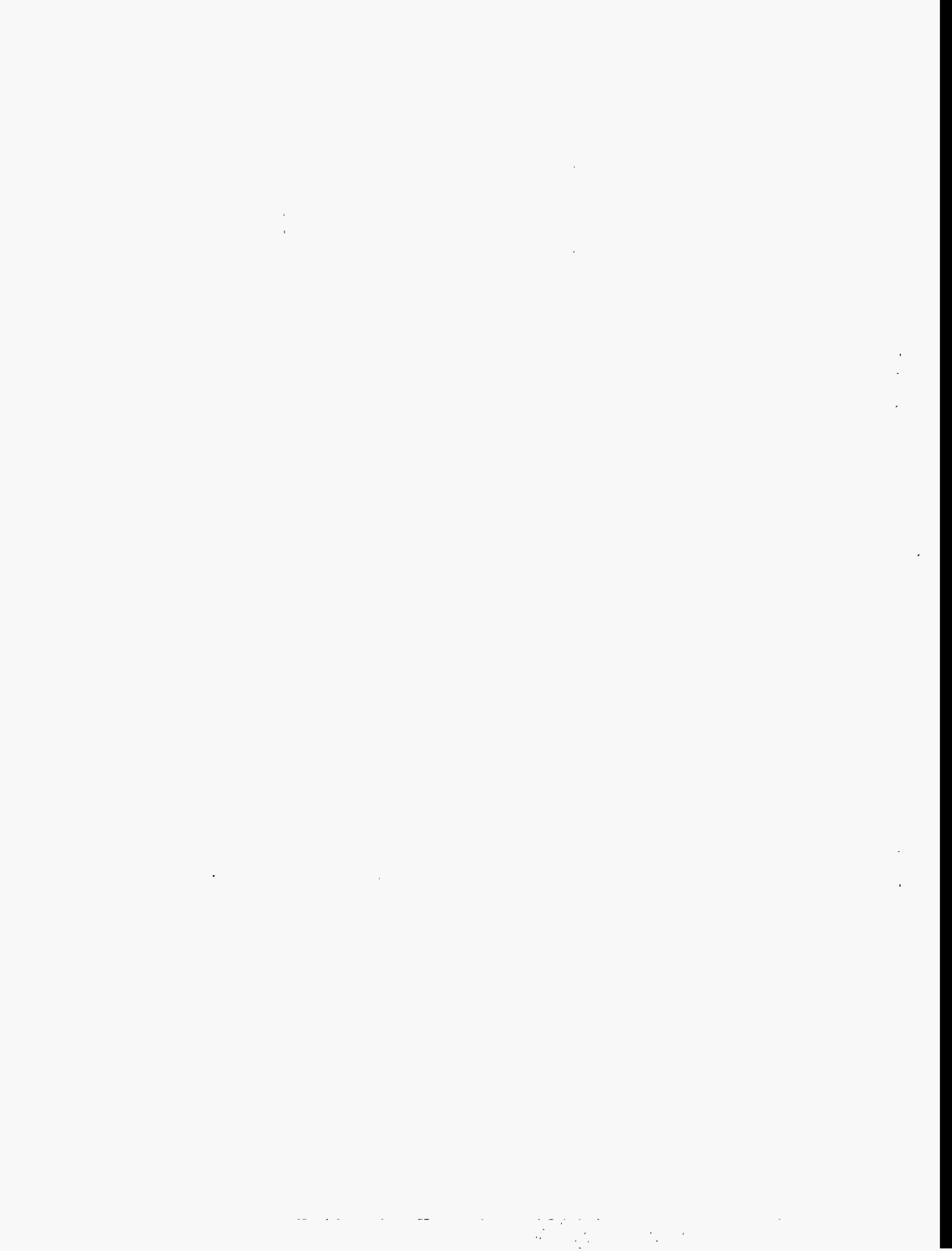
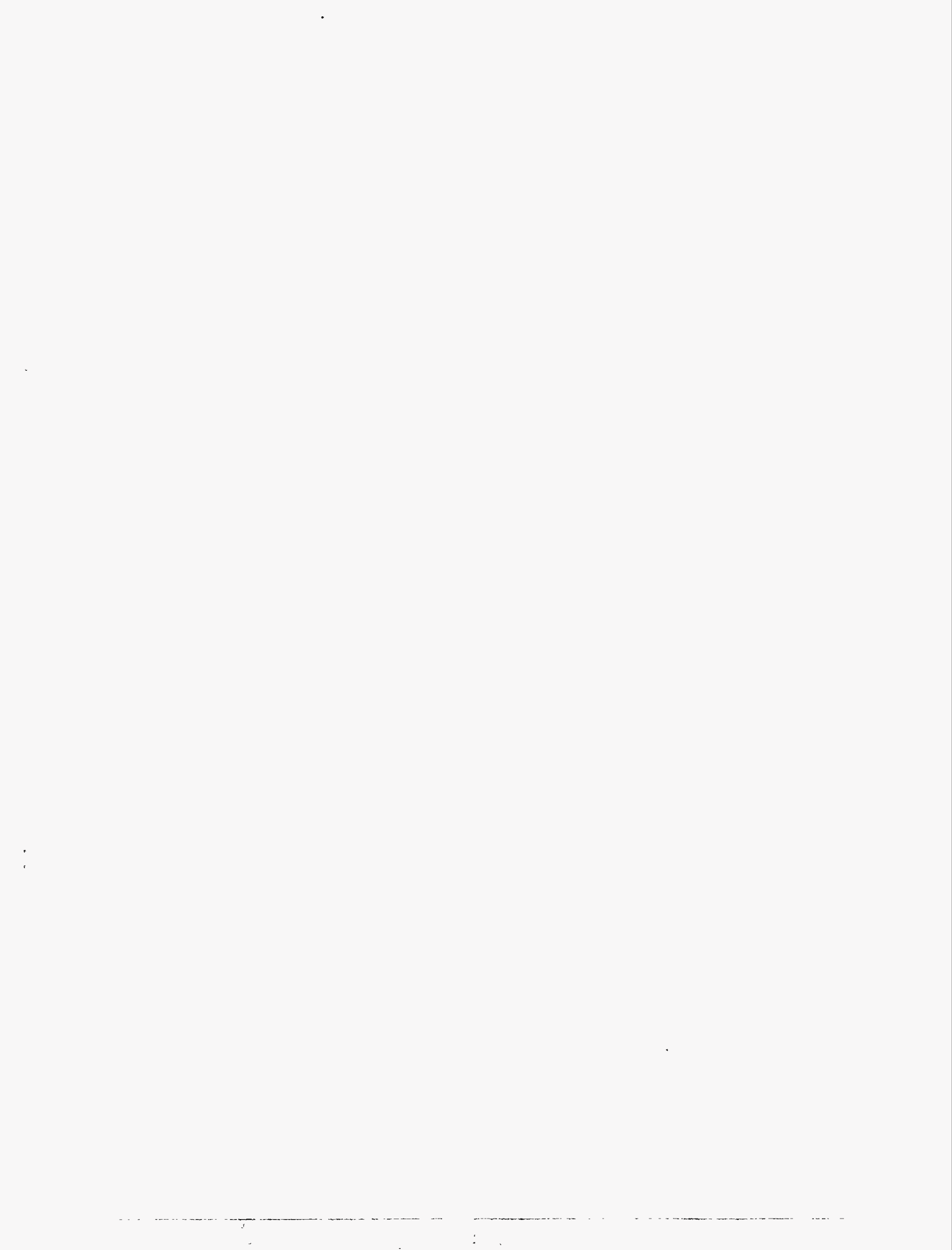


Figure 5: Electric fields for light impinging first into the seed of a nodular defect. The top trace represents the standing wave E-field (SWEF) in an ideal $\text{HfO}_2/\text{SiO}_2$ HR stack. The bottom trace is the SWEF along the center axis of the nodular defect. The E-field has decayed significantly by the time light reaches the seed. The seed did increase the local E-field maxima.





Technical Information Department • Lawrence Livermore National Laboratory
University of California • Livermore, California 94551

• • •

